The Journal of Veterinary Medical Science

NOTE

Surgery

New clinical application of three-dimensional-printed polycaprolactone/β-tricalcium phosphate scaffold as an alternative to allograft bone for limb-sparing surgery in a dog with distal radial osteosarcoma

Seongjae CHOI[1)#], Ye-In OH[2)#], Keun-Ho PARK[3)], Jeong-Seok LEE[3)], Jin-Hyung SHIM[3)*] and Byung-Jae KANG[1)*]

[1)]Department of Veterinary Surgery, College of Veterinary Medicine and Institute of Veterinary Science, Kangwon National University, Chuncheon 24341, Republic of Korea
[2)]Department of Veterinary Internal Medicine, College of Veterinary Medicine, Seoul National University, Seoul 08826, Republic of Korea
[3)]Department of Mechanical Engineering, Korea Polytechnic University, Siheung 15073, Republic of Korea

ABSTRACT. Limb-sparing surgery is one of the surgical options for dogs with distal radial osteosarcoma (OSA). This case report highlights the novel application of a three-dimensional (3D)-printed patient-specific polycaprolactone/β-tricalcium phosphate (PCL/β-TCP) scaffold in limb-sparing surgery in a dog with distal radial OSA. The outcomes evaluated included postoperative gait analysis, complications, local recurrence of tumor, metastasis, and survival time. Post-operative gait evaluation showed significant improvement in limb function, including increased weight distribution and decreased asymmetry. The implant remained well in place and increased bone opacity was observed between the host bone and the scaffold. There was no complication due to scaffold or surgery. Significant improvement in limb function and quality of life was noted postoperatively. Local recurrence and pulmonary metastasis were identified at 8 weeks postoperatively. The survival time from diagnosis of OSA to death was 190 days. The PCL/β-TCP scaffold may be an effective alternative to cortical allograft in limb-sparing surgery for bone tumors.

KEY WORDS: limb-sparing, osteosarcoma, polycaprolactone/β-tricalcium phosphate, three-dimensional-printed scaffold

J. Vet. Med. Sci.
81(3): 434–439, 2019
doi: 10.1292/jvms.18-0158

Received: 20 March 2018
Accepted: 10 January 2019
Published online in J-STAGE: 18 January 2019

Osteosarcoma (OSA) accounts for 85% of all skeletal tumors in dogs and frequently affects large and giant breeds [35]. Older dogs with a median age of 7 years are more commonly affected [26, 35]. OSA typically occurs in the axial and appendicular skeleton and is more frequent in the latter. The distal radius is the predominant site affected. In appendicular OSA, limb-sparing surgery has been considered the standard of care in humans. It is also a viable alternative to limb amputation in dogs, particularly if amputation is not preferred or not indicated due to the presence of a concomitant condition, such as neurological disease or osteoarthritis [17, 35]. No difference was reported in survival time between dogs that underwent amputation combined with chemotherapy and those managed with limb-sparing surgery and chemotherapy [34].

Three-dimensional (3D)-printing technology began in the 1980s and has recently been used with a variety of materials in a wide range of medical fields, including dentistry, orthopedics, and traumatology [1]. However, reports using 3D printing technology for patient-specific prostheses are limited in veterinary medicine to date [4, 6, 12]. Polycaprolactone (PCL) is approved by the United States Food and Drug Administration for medical use, because it is biologically safe and clinically applicable. PCL has excellent biocompatibility and is therefore the most commonly used bone scaffold [20]. It has a strong crystal structure and suitable mechanical properties after manufacturing. However, it tends to gradually biodegrade through hydrolysis [8]. To compensate for this, PCL is used in combination with β-tricalcium phosphate (β-TCP), which releases calcium to aid bone formation and is more degradable and osteoconductive [37]. In addition, PCL/β-TCP has potential as a bone graft material because it has superior ability to substitute bone, induce bone regeneration, and aid bone formation, rather than using only PCL in bone defects [31]. The present

*Correspondence to: Kang, B.-J.: bjkang@kangwon.ac.kr, Shim, J.-H.: happyshim@kpu.ac.kr
#These authors contributed equally to this work.

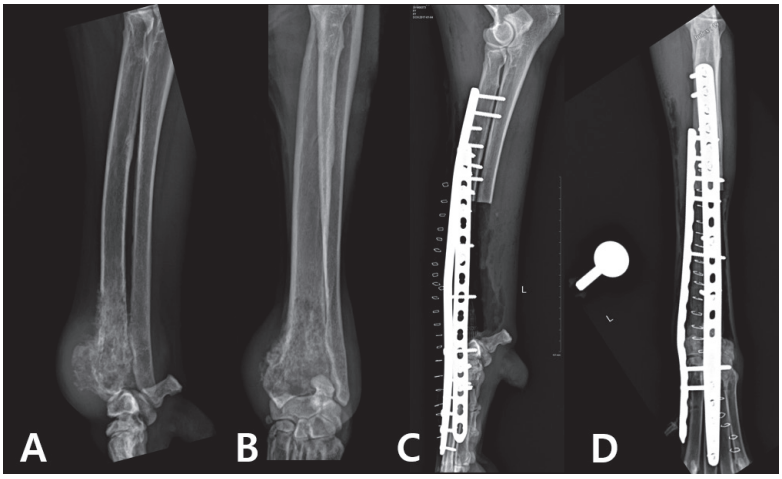

Fig. 1. (A) and (B) Preoperative mediolateral and craniocaudal radiographs demonstrating OSA of the distal radial metaphysis. (C) and (D) Immediate postoperative mediolateral and craniocaudal radiographs of limb-sparing surgery of the distal aspect of the radius using a 3D-printed PCL/β-TCP scaffold.

report is the first to present a case of distal radial OSA in a dog, treated with limb-sparing surgery using a 3D-printed PCL/β-TCP scaffold, and to evaluate its feasibility for patient-specific treatment in OSA of the distal radius.

An 8-year-old, intact female Great Pyrenees (weight: 46 kg) presented with progressive left forelimb lameness of 2 months duration and a rapidly growing palpable mass surrounding the left distal radius present for 1 month. The lameness was intermittent and of a non-weight bearing type. Physical examination of the left forelimb revealed a firm mass (5 × 8 cm) in the distal antebrachium, with signs of pain apparent on palpation of the swelling and on flexion of the carpus. Radiographic examination revealed cortical lysis and periosteal reaction of the radius and extension of osteogenesis into the adjacent soft tissue on the craniomedial aspect of the distal radius (Fig. 1A and 1B). The carpal joint appeared unremarkable. Three-view thoracic radiography and whole-body computed tomography (CT) did not reveal any evidence of metastatic disease. A cytological examination of the mass was performed through fine needle aspiration (FNA) under ultrasound guidance. Characteristic giant multinucleated cells, osteoblasts, pleomorphic mesenchymal cells with indistinct cell borders, and the intercellular eosinophilic matrix were observed. Based on these results, OSA was suspected. Complete blood count and serum biochemistry results did not reveal any abnormalities, except for a slight elevation (230 U/*l*; reference rage 23–212 U/*l*) in serum alkaline phosphatase (ALP) level.

The owner opted for limb-sparing surgery rather than amputation, considering the quality of life (QOL) of the patient, but declined all chemotherapy, including neoadjuvant and adjuvant chemotherapy. We were unable to obtain an allograft bone of the size needed for the patient, so we decided to use a 3D-printed scaffold that had already proven mechanical properties instead [2]. The 3D-printed scaffold was produced using a mixture of powdered PCL (Evonik Industry, Essen, Germany) and β-TCP (Berkeley Advanced Biomaterials Inc., Berkeley, CA, U.S.A.) and by mirroring the structure of the contralateral limb on CT (Fig. 2). Using a microextrusion-based 3D printer (3DX Printer, T&R Biofab Co., Siheung, Korea), the scaffold was fabricated using a heating process. The mixture was placed in a steel syringe with nozzle and loaded in the printer. The molten mixture was extruded by regulated pneumatic pressure. The x- and y-axes were controlled by a linear guide and linear encoder, and a ball screw was used to control the z-axis. The extruded mixture was stacked-up to fabricate the scaffold and cooled at room temperature (18°C). The inner architecture was designed to be fully interconnected and composed of blended PCL and β-TCP [12].

The limb-sparing surgery was performed through a craniomedial approach to the radius. The capsulated tumor tissue was isolated from the carpal joint without injury. Then, a transverse osteotomy was performed on the radius and ulna at a 3-cm margin from the tumor tissue using an oscillating saw in order to resect the tumor en bloc with all contiguous tissue, including the soft tissue. In a previous study, it was reported that preserving the ulna when using an allograft or endoprosthesis for limb-sparing surgery conveys no biomechanical advantage [18]. In this case, preoperative radiographic examination revealed that the OSA in the distal radius had invaded the distal ulna (Fig. 1A and 1B). Therefore, the transverse osteotomy was also performed on the distal ulna. The excised tissue was submitted for histopathological evaluation. After the osteotomy, bone marrow samples were collected from the proximal radius, and cytology performed showed that the margin was clear. The articular cartilage of the carpal and carpometacarpal joints was then removed with a high-speed burr. Since the cross-section of the radius is anatomically oval, we were able to precisely align the 3D-printed scaffold with the corresponding portion of the radius, and confirmed the position after placement. We also confirmed the alignment of the joints when we placed the scaffold against the joint surface. A 16-hole, 3.5-mm locking compression plate (Veterinary LCP, DePuy Synthes™, Oberdorf, Switzerland) was applied to the medial side, and a 21-hole 3.5/2.7 mm pancarpal arthrodesis plate (Veterinary Instrumentation, Sheffield, U.K.) was applied to the cranial aspect of the remaining radius, radial carpal bone, and third metacarpal bone according to the standard arthrodesis technique (Fig. 3) [32]. One cubic centimeter each of 2–4 mm cancellous chips (Veterinary Tissue Bank Ltd., Wrexham, U.K.) and 0.5–1.0 mm demineralized

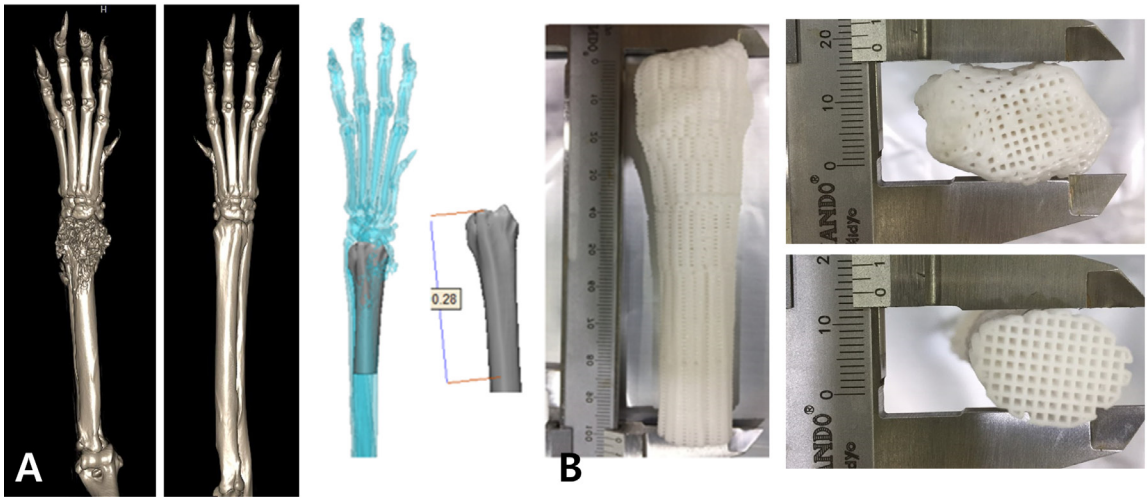

Fig. 2. 3D-printed PCL/β-TCP scaffold produced by mirroring the structure of the contralateral limb CT for distal radial limb-sparing surgery in a dog. (A) Designed 3D-scaffold using the 3D CT reconstruction image of the bilateral forelimb. (B) 3D-printed PCL/β-TCP scaffold.

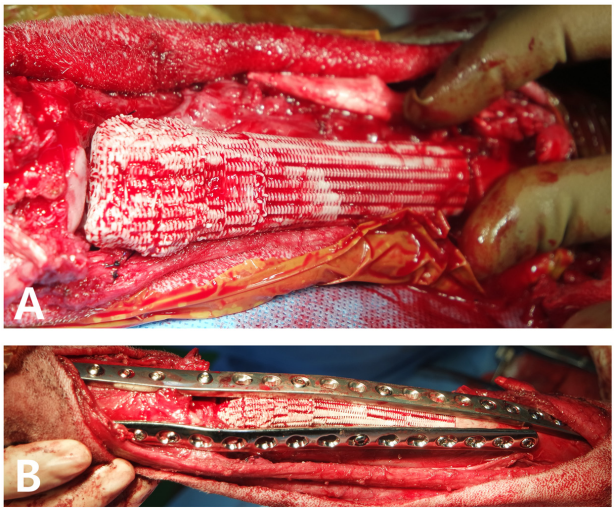

Fig. 3. Intraoperative image of limb-sparing surgery of the distal aspect of the radius using a 3D-printed PCL/β-TCP scaffold. (A) Positioning the 3D-printed scaffold at the location where the distal radius and OSA were removed. (B) Double plating for pancarpal arthrodesis with the 3D-printed PCL/β-TCP scaffold.

bone matrix (Veterinary Tissue Bank Ltd.), in addition to 1 mg of recombinant human bone morphogenetic protein-2 (rhBMP-2) (Novosis, Daewoong Co, Gyeonggi-do, Korea), was applied to the periphery of the inserted scaffold to aid in osteogenesis. A standard wound closure procedure then followed.

Immediate postoperative radiographs demonstrated proper limb alignment and implant positioning (Fig. 1C and 1D). Histopathology of the excised bone segment confirmed the diagnosis of OSA (IDEXX Reference Laboratories, Westbrook, ME, U.S.A.). However, the histopathological assessment of the margin of resected tissue was not performed, because we thought at the time that evaluation with cytology and CT provided sufficient surgical margin for tumor removal. Now, however, we think that we should have histopathologically confirmed the margin of removed tissue to confirm that we had had enough of the method we evaluated for the surgical margin. The assessment of surgical outcomes included postoperative gait analysis using the Tekscan walkway system (Tekscan, Boston, MA, U.S.A.) and the presence, severity, and time to onset of complications. The assessment of oncological outcomes included the presence and time to onset of local recurrence or metastasis and survival time.

An increase in the weight bearing force of the left forelimb was confirmed by the objective values of the pressure sensor platform gait analysis (Table 1). A symmetry index for peak vertical force and vertical impulse was used in this case to determine variations between normal and pathological gaits and thereby assess changes in asymmetry due to improvements in the pathological state. The symmetry index was calculated using the following formula [36]: Symmetry index (%)=100−[(Fl/Fc) × 100] (Fl=parameter of the lame extremity and Fc=parameter of the contralateral extremity). A significant improvement in weight bearing of the limb was noted postoperatively. Before the surgery, we were unable to evaluate the gait using the sensor because the dog's pain was severe enough to prevent weight-bearing.

Three weeks after surgery, the lameness in the left forelimb of the patient improved to a weight-bearing lameness. Visible

Table 1. Weight distribution and symmetric index data of peak vertical force (PVF) and vertical impulse (VI) for forelimbs

	3 weeks		6 weeks		8 weeks		10 weeks		4 months	
	LF	RF	LF	RF	LF	RF	LF	RF	LF	RF
Weight distribution of PVF (%)	23.25	35.85	26.99	32.79	23.92	37.96	20.07	38.69	28.29	34.38
Weight distribution of VI (%)	19.63	36.70	22.77	33.86	20.51	38.34	15.62	46.28	27.31	34.41
Symmetric index of PVF (%)	42.65		19.40		45.37		63.39		19.41	
Symmetric index of VI (%)	60.61		39.19		60.61		99.07		23.03	

LF=left forelimb; RF=right forelimb.

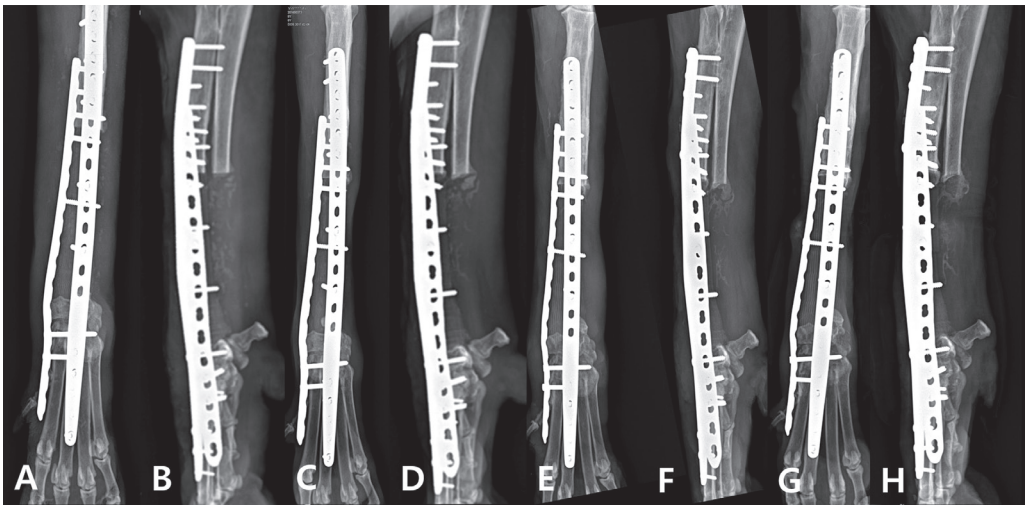

Fig. 4. Postoperative mediolateral and craniocaudal radiographs. (A) and (B) 3-week follow-up. (C) and (D) 6-week follow-up. (E) and (F) 10-week follow-up. (G) and (H) 4-month follow-up with increased opacity on the medial and caudal site of the scaffold.

improvement in lameness was noted at 6 weeks after surgery, and the radiological evaluation confirmed that the implant was well maintained and an area of increased bone opacity between the proximal radius and PCL/β-TCP scaffold (Fig. 4C and 4D). Local tumor recurrence and pulmonary metastasis were confirmed at 8 weeks postoperatively (Supp. Fig. 1). At that time, a decrease in the weight-bearing force of the left forelimb was noted and was likely due to tumor recurrence. At 10 weeks postoperatively, the lameness worsened, but gradually improved after the administration of a non-steroidal anti-inflammatory drug. At 4 months postoperatively no lameness was observed and the implant remained in place. On the lateral radiographical view of the left forelimb, a crack was identified at middle point of the 3D-printed scaffold, an area of increased opacity was identified at the distal portion of the cut ulna, and a firm mass was identified during palpation (Fig. 4G and 4H). FNA sampling of the mass revealed the presence of spindle cells, which suggested the presence of malignancy, but did not confirm OSA.

Postoperative acute and chronic complications were not observed. The survival time from diagnosis of OSA to death was 190 days. The cause of death was unclear, and post-mortem histopathological evaluation of the 3D-printed scaffold was not performed, since the owner did not opt for a necropsy of the dog.

Several studies have reported cases of cortical allograft use in limb-sparing surgery in dogs [13, 16, 21]. However, except in the United States and some European countries, allograft bone is not easily obtained because there is no bone bank for animals. The use of a 3D-printed scaffold is advantageous in such cases, as it can be obtained without a bone bank and customized to match various shapes of bone defects that arise after tumor resection [38]. The 3D-printed scaffolds are generally applied in surgery of the maxillofacial bones or vertebrae in cases of bone defects in humans and dogs [10, 12, 27]. To our knowledge, this is the first report of a case in which a biodegradable 3D-printed scaffold was applied to a limb bone where weight-bearing force was applied in a dog. No such cases have been reported in human medicine.

Common complications of limb-sparing surgery include infection, local tumor recurrence, implant failure, and stress fracture [14, 32, 35]. Infections occurring postoperatively are considered difficult to manage owing to the relative lack of blood supply to the distal antebrachium [32]. However, such complications can be reduced with a 3D-printed scaffold, which has a customizable porous structure. It has been reported that a microscale porous structure optimizes bone healing and vascular infiltration [24]. Moreover, interconnected internal pores support the infiltration of neotissues and transportation of fluidic nutrients [15]. Therefore, patients with 3D-printed scaffolds might be less susceptible to postoperative complications, such as infection. Furthermore, a tight interface between the scaffold and host tissue can be obtained, and tissue ingrowth can be promoted [23]. The 3D-printed scaffolds can be fabricated with scaffold lattices that may facilitate osteointegration and reduce implant stiffness. Modifying the porosity and pore size in the implants may further minimize the stress-shielding problem [9]. In this case, we performed customized patient

treatment using biocompatible scaffold, which was helpful in improving gait status after surgery. When PCL/β-TCP was used for maxillary bone defects in a dog, no complication were reported, and none were noted in this patient either [12]. However, in this case, since the location of applied scaffold was limb bone where weight-bearing force was applied in dogs, there may have been the possibility of a scaffold fracture before the osteointegration has been fully completed.

The dog in this case report had local recurrence and metastasis at 8 weeks postoperatively. This may be due to lack of neoadjuvant and adjuvant chemotherapy. In canine OSA, metastasis is very common, with approximately 90% death within 1 year after diagnosis [5, 33]. Because chemotherapy is beneficial in OSA, chemotherapy should be combined surgery as much as possible to reduce the possibility of recurrence or metastasis [35]. Incomplete surgical removal may also be the cause. Although we resected tumor tissue at 3 cm-margin from the tumor tissue and clear surgical margin was confirmed by the cytology of the resected site, we cannot exclude the possibility that surgical margin was not clear because of inaccuracy in cytology more than histopathology. rhBMP-2 can be considered as another reason of early recurrence and metastasis. Although rhBMP-2 has been shown to increase cancer risk in humans, whether or not rhBMP-2 affects recurrence and metastasis is still controversial [19, 28, 39]. Further studies are required to evaluate whether tumor recurrence and metastasis may be reduced by adding an anticancer agent to the 3D-printed scaffold.

Serum ALP is a strong negative prognostic factor for canine OSA [3]. In general, dogs with high ALP values before surgery have a shorter survival time (hazard ratio of 1.62, 95% CI: 1.21–2.17) and disease-free interval (hazard ratio of 1.96, 95% CI: 1.50–2.56) [3, 25, 29]. Although slightly elevated ALP levels were noted in this case, the owner opted for limb-sparing surgery to improve the QOL during the patient's survival period. The patient survived for 5 months (160 days) after surgery without chemotherapy. The median survival time for dogs with appendicular OSA, after amputation alone, is approximately 5 months, and the 1-year survival rate is 11% [33]. The median survival time for dogs receiving adjuvant chemotherapy with amputation is 1 year, regardless of the protocol used [7]. Therefore, the survival time of the patient in this case was not less than previously reported values. Moreover, the owner was satisfied that limb-sparing surgery with the 3D-printed scaffold improved the patient's QOL without amputation. The dog likely would have survived longer if chemotherapy had been added.

In our study, an area of increased opacity suggestive of bone regeneration was confirmed between the proximal radius and PCL/β-TCP scaffold at 6 weeks post-surgery on radiographs. However, since the bone was not evaluated histologically, it was not confirmed whether the bone was integrated from the radial section and had connectivity with the scaffold. Previous studies have reported excellent new bone formation abilities in animals using a PCL/β-TCP scaffold for treating bone defects [30, 31]. PCL/β-TCP can increase compressive strength and improve cell and tissue integration [11, 30]. In addition, 3D-printed scaffolds have a pore structure that may facilitate osteointegration. There is a limitation in this study that long-term follow-up of scaffold was not possible because the patient died within 6 months postoperatively. However, previous study has shown long-term stability of this material in the body [22]. Tissues showed ingrowth from the 3-dimensional interconnected pores inside the scaffold, degradating and getting substituted by surrounding tissues. Likewise, the PCL/TCP scaffold implanted in this study was in a more positive environment for osteogenesis because bones were the surrounding tissues and it was rich in bone marrow. Therefore, biodegradation of the TCP will be accompanied by bone regeneration inside the body. Even if the TCP is degradated, the PCL polymer maintains strength inside the body for a certain period. In our study, the weight-bearing force of the patient's left forelimb was increased without implant failure for approximately 6 months until the patient died. Therefore, it is expected that bone union between the proximal radius and the carpus to the PCL/β-TCP scaffold had occurred and stability was acquired.

This is the first case where a 3D-printed scaffold was used successfully in limb-sparing surgery of a dog. This procedure can be used to improve the QOL of patients for which allografts cannot be obtained. We conclude that a 3D-printed PCL/β-TCP scaffold can be used as an alternative to cortical allograft for bone reconstruction and may improve the effectiveness of limb-sparing surgery for bone tumors.

ACKNOWLEDGMENTS. This study was supported by the Basic Science Research Program through the National Research Foundation of Korea (NRF) funded by the Ministry of Science, ICT & Future Planning (NRF-2015R1C1A1A01051759 and NRF-2017R1A6A1A03015562).

REFERENCES

1. Auricchio, F. and Marconi, S. 2017. 3D printing: clinical applications in orthopaedics and traumatology. *EFORT Open Rev* **1**: 121–127. [Medline] [CrossRef]
2. Bae, J. C., Lee, J. J., Shim, H. H., Park, K. H., Lee, J. S., Bae, E. B., Choi, J. W. and Huh, J. B. 2017. Development and assessment of a 3D-printed scaffold with rhBMP-2 for an implanted surgical guide stent and bone graft material: a pilot animal study. *Materials (Basel)* **10**: 1434–1454. [CrossRef]
3. Boerman, I., Selvarajah, G. T., Nielen, M. and Kirpensteijn, J. 2012. Prognostic factors in canine appendicular osteosarcoma - a meta-analysis. *BMC Vet. Res.* **8**: 56–67. [Medline] [CrossRef]
4. Bray, J. P., Kersley, A., Downing, W., Crosse, K. R., Worth, A. J., House, A. K., Yates, G., Coomer, A. R. and Brown, I. W. M. 2017. Clinical outcomes of patient-specific porous titanium endoprostheses in dogs with tumors of the mandible, radius, or tibia: 12 cases (2013–2016). *J. Am. Vet. Med. Assoc.* **251**: 566–579. [Medline] [CrossRef]
5. Brodey, R. S. and Riser, W. H. 1969. Canine osteosarcoma. A clinicopathologic study of 194 cases. *Clin. Orthop. Relat. Res.* **62**: 54–64. [Medline]
6. Castilho, M., Dias, M., Vorndran, E., Gbureck, U., Fernandes, P., Pires, I., Gouveia, B., Armés, H., Pires, E. and Rodrigues, J. 2014. Application of a 3D printed customized implant for canine cruciate ligament treatment by tibial tuberosity advancement. *Biofabrication* **6**: 025005. [Medline] [CrossRef]

7. Dobson, J. M. and Lascelles, B. D. X. 2011. BSAVA Manual of Canine and Feline Oncology, British Small Animal Veterinary Association, Gloucester.
8. Eshraghi, S. and Das, S. 2010. Mechanical and microstructural properties of polycaprolactone scaffolds with one-dimensional, two-dimensional, and three-dimensional orthogonally oriented porous architectures produced by selective laser sintering. *Acta Biomater.* **6**: 2467–2476. [Medline] [CrossRef]
9. Harrysson, O. L., Cansizoglu, O., Marcellin-Little, D. J., Cormier, D. R. and West, H. A. II. 2008. Direct metal fabrication of titanium implants with tailored materials and mechanical properties using electron beam melting technology. *Mater. Sci. Eng. C Biomim. Supramol. Syst.* **28**: 366–373.
10. Khojasteh, A., Behnia, H., Hosseini, F. S., Dehghan, M. M., Abbasnia, P. and Abbas, F. M. 2013. The effect of PCL-TCP scaffold loaded with mesenchymal stem cells on vertical bone augmentation in dog mandible: a preliminary report. *J. Biomed. Mater. Res. B Appl. Biomater.* **101**: 848–854. [Medline] [CrossRef]
11. Kim, J. Y., Yoon, J. J., Park, E. K., Kim, D. S., Kim, S. Y. and Cho, D. W. 2009. Cell adhesion and proliferation evaluation of SFF-based biodegradable scaffolds fabricated using a multi-head deposition system. *Biofabrication* **1**: 015002. [Medline] [CrossRef]
12. Kim, S. E., Shim, K. M., Jang, K., Shim, J. H. and Kang, S. S. 2018. Three-dimensional printing-based reconstruction of a maxillary bone defect in a dog following tumor removal. *In Vivo* **32**: 63–70. [Medline]
13. Kirpensteijn, J., Steinheimer, D., Park, R., Powers, B., Straw, R., Endenburg, N. and Withrow, S. 1998. Comparison of cemented and non-cemented allografts in dogs with osteosarcoma. *Vet. Comp. Orthop. Traumatol.* **11**: 178–184. [CrossRef]
14. Lascelles, B. D. X., Dernell, W. S., Correa, M. T., Lafferty, M., Devitt, C. M., Kuntz, C. A., Straw, R. C. and Withrow, S. J. 2005. Improved survival associated with postoperative wound infection in dogs treated with limb-salvage surgery for osteosarcoma. *Ann. Surg. Oncol.* **12**: 1073–1083. [Medline] [CrossRef]
15. Lee, J. W., Kang, K. S., Lee, S. H., Kim, J. Y., Lee, B. K. and Cho, D. W. 2011. Bone regeneration using a microstereolithography-produced customized poly(propylene fumarate)/diethyl fumarate photopolymer 3D scaffold incorporating BMP-2 loaded PLGA microspheres. *Biomaterials* **32**: 744–752. [Medline] [CrossRef]
16. Liptak, J. M., Dernell, W. S., Ehrhart, N., Lafferty, M. H., Monteith, G. J. and Withrow, S. J. 2006. Cortical allograft and endoprosthesis for limb-sparing surgery in dogs with distal radial osteosarcoma: a prospective clinical comparison of two different limb-sparing techniques. *Vet. Surg.* **35**: 518–533. [Medline] [CrossRef]
17. Liptak, J. M. F., Dernell, W. S., Ehrhart, N., Withrow, S. J., Séguin, B., Walsh, P. J. and Kuntz, C. A. 2004. Canine appendicular osteosarcoma: curative-intent treatment. *Compend. Contin. Educ. Pract. Vet.* **26**: 186–197.
18. Liptak, J. M., Dernell, W. S., Lascelles, B. D. X., Larue, S. M., Jameson, V. J., Powers, B. E., Huber, D. J. and Withrow, S. J. 2004. Intraoperative extracorporeal irradiation for limb sparing in 13 dogs. *Vet. Surg.* **33**: 446–456. [Medline] [CrossRef]
19. Low, J., Ross, J. S., Ritchie, J. D., Gross, C. P., Lehman, R., Lin, H., Fu, R., Stewart, L. A. and Krumholz, H. M. 2017. Comparison of two independent systematic reviews of trials of recombinant human bone morphogenetic protein-2 (rhBMP-2): the Yale Open Data Access Medtronic Project. *Syst. Rev.* **6**: 28–36. [Medline] [CrossRef]
20. Lu, L., Zhang, Q., Wootton, D., Chiou, R., Li, D., Lu, B., Lelkes, P. and Zhou, J. 2012. Biocompatibility and biodegradation studies of PCL/β-TCP bone tissue scaffold fabricated by structural porogen method. *J. Mater. Sci. Mater. Med.* **23**: 2217–2226. [Medline] [CrossRef]
21. Morello, E., Buracco, P., Martano, M., Peirone, B., Capurro, C., Valazza, A., Cotto, D., Ferracini, R. and Sora, M. 2001. Bone allografts and adjuvant cisplatin for the treatment of canine appendicular osteosarcoma in 18 dogs. *J. Small Anim. Pract.* **42**: 61–66. [Medline] [CrossRef]
22. Park, S. H., Yun, B. G., Won, J. Y., Yun, W. S., Shim, J. H., Lim, M. H., Kim, D. H., Baek, S. A., Alahmari, Y. D., Jeun, J. H., Hwang, S. H. and Kim, S. W. 2017. New application of three-dimensional printing biomaterial in nasal reconstruction. *Laryngoscope* **127**: 1036–1043. [Medline] [CrossRef]
23. Peroglio, M., Gremillard, L., Eglin, D., Lezuo, P., Alini, M. and Chevalier, J. 2010. Evaluation of a new press-fit in situ setting composite porous scaffold for cancellous bone repair: towards a "surgeon-friendly" bone filler? *Acta Biomater.* **6**: 3808–3812. [Medline] [CrossRef]
24. Peters, M. C., Polverini, P. J. and Mooney, D. J. 2002. Engineering vascular networks in porous polymer matrices. *J. Biomed. Mater. Res.* **60**: 668–678. [Medline] [CrossRef]
25. Phillips, B., Powers, B. E., Dernell, W. S., Straw, R. C., Khanna, C., Hogge, G. S. and Vail, D. M. 2009. Use of single-agent carboplatin as adjuvant or neoadjuvant therapy in conjunction with amputation for appendicular osteosarcoma in dogs. *J. Am. Anim. Hosp. Assoc.* **45**: 33–38. [Medline] [CrossRef]
26. Ru, G., Terracini, B. and Glickman, L. T. 1998. Host related risk factors for canine osteosarcoma. *Vet. J.* **156**: 31–39. [Medline] [CrossRef]
27. Ryan, G., Pandit, A. and Apatsidis, D. P. 2006. Fabrication methods of porous metals for use in orthopaedic applications. *Biomaterials* **27**: 2651–2670. [Medline] [CrossRef]
28. Sayama, C., Willsey, M., Chintagumpala, M., Brayton, A., Briceño, V., Ryan, S. L., Luerssen, T. G., Hwang, S. W. and Jea, A. 2015. Routine use of recombinant human bone morphogenetic protein-2 in posterior fusions of the pediatric spine and incidence of cancer. *J. Neurosurg. Pediatr.* **16**: 4–13. [Medline] [CrossRef]
29. Selvarajah, G. T., Kirpensteijn, J., van Wolferen, M. E., Rao, N. A., Fieten, H. and Mol, J. A. 2009. Gene expression profiling of canine osteosarcoma reveals genes associated with short and long survival times. *Mol. Cancer* **8**: 72–89. [Medline] [CrossRef]
30. Shim, J. H., Moon, T. S., Yun, M. J., Jeon, Y. C., Jeong, C. M., Cho, D. W. and Huh, J. B. 2012. Stimulation of healing within a rabbit calvarial defect by a PCL/PLGA scaffold blended with TCP using solid freeform fabrication technology. *J. Mater. Sci. Mater. Med.* **23**: 2993–3002. [Medline] [CrossRef]
31. Shim, J. H., Won, J. Y., Park, J. H., Bae, J. H., Ahn, G., Kim, C. H., Lim, D. H., Cho, D. W., Yun, W. S., Bae, E. B., Jeong, C. M. and Huh, J. B. 2017. Effects of 3D-printed polycaprolactone/β-tricalcium phosphate membranes on guided bone regeneration. *Int. J. Mol. Sci.* **18**: 899–914. [Medline] [CrossRef]
32. Slatter, D. H. 2003. Textbook of Small Animal Surgery, Elsevier Health Sciences, London.
33. Spodnick, G. J., Berg, J., Rand, W. M., Schelling, S. H., Couto, G., Harvey, H. J., Henderson, R. A., MacEwen, G., Mauldin, N., McCaw, D. L., *et al*. 1992. Prognosis for dogs with appendicular osteosarcoma treated by amputation alone: 162 cases (1978–1988). *J. Am. Vet. Med. Assoc.* **200**: 995–999. [Medline]
34. Straw, R. C. and Withrow, S. J. 1996. Limb-sparing surgery versus amputation for dogs with bone tumors. *Vet. Clin. North Am. Small Anim. Pract.* **26**: 135–143. [Medline] [CrossRef]
35. Vail, D. M. and Page, R. L. 2013. Withrow & MacEwen's Small Animal Clinical Oncology, Elsevier Saunders, St. Louis.
36. Volstad, N. J., Sandberg, G., Robb, S. and Budsberg, S. C. 2017. The evaluation of limb symmetry indices using ground reaction forces collected with one or two force plates in healthy dogs. *Vet. Comp. Orthop. Traumatol.* **30**: 54–58. [Medline] [CrossRef]
37. Vorndran, E., Klarner, M., Klammert, U., Grover, L. M., Patel, S., Barralet, J. E. and Gbureck, U. 2008. 3D powder printing of β-tricalcium phosphate ceramics using different strategies. *Adv. Eng. Mater.* **10**: B67–B71. [CrossRef]
38. Wong, K. C., Kumta, S. M., Geel, N. V. and Demol, J. 2015. One-step reconstruction with a 3D-printed, biomechanically evaluated custom implant after complex pelvic tumor resection. *Comput. Aided Surg.* **20**: 14–23. [Medline] [CrossRef]
39. Zaid, K. W., Chantiri, M. and Bassit, G. 2016. Recombinant human bone morphogenetic protein-2 in development and progression of oral squamous cell carcinoma. *Asian Pac. J. Cancer Prev.* **17**: 927–932. [Medline] [CrossRef]